CHEMISTRY OF MATERIALS
Article

Chem. Mater. **2009,** *21,* 4323–4331 4323
DOI:10.1021/cm9023474

Surface-Tethered pH-Responsive Hydrogel Thin Films as Size-Selective Layers on Nanoporous Asymmetric Membranes

Wyatt E. Tenhaeff and Karen K. Gleason*

Department of Chemical Engineering Institute for Soldier Nanotechnologies Massachusetts Institute of Technology 77 Massachusetts Avenue Cambridge, Massachusetts 02139

Received June 18, 2009

The fabrication of prototype composite membranes consisting of permeable, size-selective hydrogel thin films on porous alumina membrane supports is described. Smooth hydrogel films with sub-100 nm thicknesses lacking micrometer-sized pinholes were readily synthesized using initiated chemical vapor deposition (iCVD). iCVD was a convenient technique for membrane applications as it enabled control over the coating conformality by modulating surface concentrations of the polymer precursors and film thickness through in situ monitoring of the deposition process. Scanning electron microscopy confirmed that the deposited film bridged the pore openings of the alumina supports, and little pore infiltration occurred. Membrane permeability was controlled through variation of the thickness and composition of the iCVD poly[maleic anhydride-co-dimethylacrylamide-co-di(ethylene glycol) di(vinyl ether)] (PMaDD) film. The combination of swelling and stability was achieved for a film composition of 76% N,N-dimethyl acrylamide, 14% maleic anhydride, and 10% di(ethylene glycol) divinyl ether. Swelling was shown to be pH-responsive, with a maximum swelling ratio of 11.5 at pH 8, which is a significant improvement over previous iCVD-deposited hydrogels. Hydrogel nanofilms reached their swelling equilibrium in a few minutes. Diffusion and selectivity of permeants in the membrane were also modeled and characterized. The hydrogel's internal pore size was calculated to be 3.2 nm at pH 7, which readily allowed the passage of glucose while excluding bovine serum albumin (BSA). Techniques to graft films to the substrates have been developed. By reacting 3-aminopropyldimethylethoxysilane with silanol groups of silicon surfaces and the alumina hydroxide of alumina surfaces, covalent bonds between the substrates and anhydride functionalities in the hydrogels were formed, which was necessary for stable adhesion. Further utility of PMaDD was demonstrated by functionalizing it with 2-aminoethanethiol and poly(ethylene glycol) to modulate its interaction with proteins in solution. A simple technique to pattern the film was demonstrated, and PMaDD was functionalized with CdSe/ZnS core−shell quantum dots to reveal the hydrogel properties of the patterns.

1. Introduction

Membrane separations are critical to the successful, efficient operation of many commercial processes, such as kidney dialysis, pharmaceutical purification, gas separation, and water desalination.[1−5] A key motivation for using membranes is the separation selectivity. To be economically feasible, though, the permeability (throughput) of the membrane must also be high. The selectivity and permeability characteristics are paramount, but the membrane must meet many other requirements: mechanical stability, chemical stability, and environmental compatibility of the surface, for example. Developing a single material to satisfy all these requirements is difficult. A common solution is the development of composite membranes consisting of a highly permeable porous bulk material that provides mechanical strength and a thin permselective skin layer on top for selectivity and proper interfacial properties.[6]

Innovative techniques have been developed to synthesize these skin layers; the Loeb−Sourirajan Process, interfacial polymerization, and solution coating are the most common.[7] These skin layers must be as thin as possible to maximize permeability. To synthesize high-quality, defect-free layers with these conventional methods, thicknesses greater than 1 μm are typically required.[8] Furthermore, the layer should also be readily chemically functionalized to control undesired fouling and impart new functionality, such as enhanced selectivity or stimuli-responsiveness.

*kkgleasn@mit.edu.

(1) Bernardo, P.; Drioli, E.; Golemme, G. *Ind. Eng. Chem. Res.* **2009**, *48*, 4638–4663.
(2) Kawakami, H. *J. Artif. Organs* **2008**, *11*, 177–181.
(3) Oh, J. K.; Drumright, R.; Siegwart, D. J.; Matyjaszewski, K. *Prog. Polym. Sci.* **2008**, *33*, 448–477.
(4) Shannon, M. A.; Bohn, P. W.; Elimelech, M.; Georgiadis, J. G.; Marinas, B. J.; Mayes, A. M. *Nature* **2008**, *452*, 301–310.
(5) Stamatialis, D. F.; Papenburg, B. J.; Girones, M.; Saiful, S.; Bettahalli, S. N. M.; Schmitmeier, S.; Wessling, M. *J. Membr. Sci.* **2008**, *308*, 1–34.
(6) Ulbricht, M. *Polymer* **2006**, *47*, 2217–2262.
(7) Baker, R. W., *Membrane Technology and Applications*. Wiley: Chichester, U.K., 2004.
(8) Pinnau, I.; Freeman, B. D.\ Formation and modification of polymeric membranes: overview. In *Membrane Formation and Modification*; Pinnau, I., Freeman, B. D., Eds.; American Chemical Society: Washington, D.C., 2000; Vol. *744*, pp 1−22.

Published on Web 08/26/2009

Having nonfouling properties is particularly important since fouling results in reduced efficiencies. Particulate (colloidal), protein, and cellular adsorption are the common culprits. Particulates are easily separated in prefilters. A common strategy to prevent protein/cellular adsorption is making the surface hydrophilic.[9] Poly(ethylene glycol) (PEG) brushes are even more effective in repelling proteins.[10−12] It is critical that these hydrophilic modification layers be firmly attached to the membrane. Indeed, poly(vinyl pyrrolidone) layers for commercial microfiltration and ultrafiltration membranes, which are immobilized relatively weakly through physical interactions, have been shown to be washed away by shear stresses.[13]

Hydrogels, which are cross-linked polymeric networks that imbibe large volumes of water but yet do not dissolve, are potentially useful materials for these skin layers. The cross-linking density of the hydrogel and water absorption define a mesh size between cross-links in the polymer,[14−16] which enables separation based on hydrodynamic size. Moreover, many strategies exist to functionalize these materials with protein-resistant moieties, often involving the grafting of PEG brushes.[12,17] A review was also recently published on stimuli-responsive hydrogels, which could enable further control in membrane separations.[18] It is important to note that hydrogels must be integrated in composite membranes because they lack mechanical strength in the gel state.

Hydrogels are clearly convenient materials for the skin layers in composite membranes. Commercial techniques exist to synthesize cross-linked hydrophilic materials on common membrane materials.[19,20] Other novel techniques, such as layer-by-layer (LbL) depositions of polyelectrolytes and plasma polymerizations, have also been investigated.[6,9,21] However, the LbL technology is generally limited to the use of polyelectrolytes of opposing charges, and modification of internal pore walls is difficult with plasma techniques because the mean free path of the plasma is larger than the pore diameter.[6] Initiated chemical vapor deposition (iCVD) is a polymer deposition technique with a broad polymerization capability—essentially equivalent to solution-phase free radical polymerizations. A broad array of polymer chemistries has been demonstrated.[22] Furthermore, membrane pores with an aspect ratio as high as 80 have been conformally coated with the technique. iCVD is particularly useful for membrane applications as it enables precise, nanometer-level control over film thickness at high deposition rates through in situ monitoring of the deposition process using interferometry.[23] Deposition rates greater well above 100 nm/min have been demonstrated.[24−26] The LBL technique, on the other hand, is limited in potential practical applications by the numerous deposition and rinsing steps required for synthesis.[27] iCVD is also a one-step process, whereas many techniques, such as interfacial polymerizations and LBL, require rinsing steps.

Furthermore, the synthesis of defect-free selective skin layers with thicknesses less than 100 nm is extremely difficult with conventional methods.[28] The synthesis of layers with thicknesses down to 50 nm is even rarer.[29] iCVD has been applied to the synthesis of sub-100 nm thick, pH-responsive hydrogel films as skin layers on porous alumina membranes. Herein, the novel chemistry of the hydrogel film is described. Furthermore, a strategy to covalently attach the polymer to the substrate was developed to increase the stability of the film. Also, the network structure of the hydrogel was characterized and its utility for dialysis in a composite membrane format was characterized. This study is primarily concerned with describing the unique synthesis technique for these hydrogels and characterizing them as potential selective skin layers. Prototype composite membranes are fabricated to demonstrate the utility of the iCVD method; extensive membrane characterization and optimization will be reported in future work.

2. Experimental Section

2.1. Hydrogel Synthesis by iCVD. Prior to synthesizing hydrogel films, 100-mm diameter silicon (Si) wafer substrates (Wafer World, test grade) were treated with 3-aminopropyldimethylmonoethoxysilane (3-AMS) (Gelest, > 95%). Using "piranha" solution (mixture of sulfuric acid and hydrogen peroxide), the surfaces of the wafers were cleaned and oxidized to create Si−OH groups at the surface, and then rinsed with clean deionized water and dried. ***Caution****: Piranha solution is a strong oxidant and should be handled with extreme care*. The wafers were placed in a vacuum oven at 60 °C, and 3-AMS vapors were flowed into the vacuum chamber for 1 h. The flow was then stopped, and the vacuum chamber was pumped out for a minimum of 1 h to remove any physisorbed 3-AMS from the surface of the Si wafers.

(9) Wang, Z. G.; Wan, L. S.; Xu, Z. K. *J. Membr. Sci.* **2007**, *304*, 8–23.
(10) Brown, A. A.; Khan, N. S.; Steinbock, L.; Huck, W. T. S. *Eur. Polym. J.* **2005**, *41*, 1757–1765.
(11) Kingshott, P.; Griesser, H. J. *Curr. Opin. Solid State Mater. Sci.* **1999**, *4*, 403–412.
(12) Satulovsky, J.; Carignano, M. A.; Szleifer, I. *Proc. Natl. Acad. Sci. U.S.A.* **2000**, *97*, 9037–9041.
(13) Matsuda, M.; Sato, M.; Sakata, H.; Ogawa, T.; Yamamoto, K.; Yakushiji, T.; Fukuda, M.; Miyasaka, T.; Sakai, K. *J. Artif. Organs* **2008**, *11*, 148–155.
(14) Canal, T.; Peppas, N. A. *J. Biomed. Mater. Res.* **1989**, *23*, 1183.
(15) Flory, P. J.; Rehner, J. J. *J. Chem. Phys.* **1943**, *11*, 521–526.
(16) Sen, M.; Guven, O. *Polymer* **1998**, *39*, 1165–1172.
(17) Wazawa, T.; Ishizuka-Katsura, Y.; Nishikawa, S.; Iwane, A. H.; Aoyama, S. *Anal. Chem.* **2006**, *78*, 2549–2556.
(18) Tokarev, I.; Minko, S. *Soft Matter* **2009**, *5*, 511–524.
(19) Hu, H.; Cai, Z. Hydrophilic microporous polyolefin membrane. U.S. Patent 5209849, **1992**.
(20) Steuck, M.; Reading, N. Porous membrane having hydrophilic surface and process. U.S. Patent 4618533, **1984**.
(21) Bruening, M. L.; Dotzauer, D. M.; Jain, P.; Ouyang, L.; Baker, G. L. *Langmuir* **2008**, *24*, 7663–7673.
(22) Tenhaeff, W. E.; Gleason, K. K. *Adv. Funct. Mater.* **2008**, *18*, 979–992.
(23) Karaman, M.; Kooi, S. E.; Gleason, K. K. *Chem. Mater.* **2008**, *20*, 2262–2267.
(24) Gupta, M.; Gleason, K. K. *Langmuir* **2006**, *22*, 10047–10052.
(25) Gupta, M.; Kapur, V.; Pinkerton, N. M.; Gleason, K. K. *Chem. Mater.* **2008**, *20*, 1646–1651.
(26) Lau, K. K. S.; Gleason, K. K. *Macromolecules* **2006**, *39*, 3688–3694.
(27) Bruening, M.; Dotzauer, D. *Nat. Mater.* **2009**, *8*, 449–450.
(28) Hachisuka, H.; Ohara, T.; Ikeda, K.\ A new type of asymmetric polyimide gas separation membrane having ultrathin skin layer. In *Membrane Formation and Modification*; Pinnau, I., Freeman, B. D., Eds.; American Chemical Society: Washington, D.C., 2000; Vol. *744*, pp 65−78.
(29) Sullivan, D. M.; Bruening, M. L. *Chem. Mater.* **2003**, *15*, 281–287.

iCVD was performed in a previously described iCVD reactor configuration.[30] Maleic anhydride (99%), *N*,*N*-dimethylacrylamide (99%), di(ethylene glycol) di(vinyl ether) (99%), and tert-butyl peroxide (97%) were all purchased from Sigma-Aldrich and used as received. By heating the precursors to create adequate vapor pressures, flow rates of 0.6 sccm of maleic anhydride, 5.9 sccm of *N*,*N*-dimethylacrylamide, and 0.4 sccm of tert-butyl peroxide were maintained with MKS Instruments 1152C, 1150C, and 1479 MFCs, respectively. The di(ethylene glycol) di(vinyl ether) flow was set manually at 0.4 sccm with a needle valve. Systematic variation of the flow rate ratios was performed to yield highly swellable, yet stable films of poly[maleic anhydride-co-dimethyl acrylamide-co-di(ethylene glycol) divinyl ether] (PMaDD). An operating pressure of 400 mTorr was maintained during the deposition, and the filament temperature was set to 235 °C by passing 0.95 A through the Chromaloy O (Goodfellow) filament (20.3 V across the filament), which was suspended 1.5 cm above the substrate. The stage temperature was 20 °C to promote adsorption of monomers. In situ interferometry with a 633 nm HeNe laser source (JDS Uniphase) was used to deposit approximately 150 nm thick films on the Si substrates.

2.2. Film Characterization. FTIR measurements were performed on a Nicolet Nexus 870 ESP spectrometer in transmission mode. Measurements were collected from 500 to 4000 cm^{-1} with 4 cm^{-1} resolution using a DTGS KBr detector. 64 scans were integrated to improve the signal-to-noise ratio. Si wafers served as backgrounds, and spectra were normalized to thickness and baseline corrected. XPS survey and high-resolution spectra were collected on a Kratos Axis Ultra spectrometer with a monochromatized Al K source. Relative sensitivity factors were calibrated by measuring poly(2-ethyl-2-oxazoline), poly(*N*,*N*-dimethylacrylamide), and poly(*N*-isopropylacrylamide) polymers (Scientific Polymer Products) spun-cast onto Si wafers from 2-propanol. Deposition samples and standards were stored in vacuum prior to analysis.

A J. A. Woollam M-2000 spectroscopic ellipsometer was used to measure film thicknesses. All thickness measurements were performed at a 75° incidence angle using 190 wavelengths from 315 to 718 nm. A nonlinear least-squares minimization algorithm was used to fit ellipsometric data of dry films to the Cauchy−Urbach model. Film thickness and refractive index coefficients were obtained upon convergence of the algorithm. To measure water-swollen films, a liquid cell accessory was used (J.A. Woollam). The cell clamped over the sample and held the solution in a liquid tight seal. The optical properties of the cell windows and soution were included in the model. Ionic strength-controlled buffer solutions of pH from 0.5 to 9 were prepared by mixing the proper ratios phosphoric acid (50% (w/v) in water), sodium dihydrogen phosphate (99%), disodium phosphate heptahydrate (99%), and sodium chloride (99%), which were all obtained from Sigma Aldrich and used as received. The ionic strength was controlled at 30 mM and the buffer strength at 10 mM. Swollen films were modeled with the effective medium approximation. One component consisted of the dry polymer (optical properties of the dry films were used), and the second component was water. The total film thickness and volume fraction of water were determined upon convergence of the nonlinear least-squares minimization algorithm. Between each measurement, the films were removed from the liquid cell, rinsed with deionized water, and then dried.

2.3. Membrane Integration. PMaDD film was deposited on commercially available porous alumina membranes with 20 nm pore openings (Anopore, SPI Supplies). Hydroxyl functional groups are present on alumina surfaces and can be used for silanization.[31,32] Silanization of the alumina with 3-AMS and deposition of PMaDD was performed using the procedure described above. High-resolution images of the membrane cross-sections were collected using a field emission scanning electron microscope (JEOL, 6700F).

Diffusion of glucose and bovine serum albumin (BSA) through the PMaDD membranes was measured in a standard Franz diffusion cell. The volume of the source chamber was 7 mL. The volume of the sink was 170 mL for glucose measurements and 70 mL for BSA measurements. The source and sink chambers were connected through a 15 mm O-ring joint. The composite membranes were sandwiched between two o-rings. Solutions of known BSA and glucose concentrations were prepared in the pH 7 buffer described above and then loaded into the source chamber. The sink was initially pure buffer. Aliquots were collected as a function of time. Glucose concentrations were measured using a blood glucose monitor (WaveSense Presto, Agamatrix, Inc.). BSA concentrations were quantified using the Coomassie Plus Protein Assay (Pierce Protein Research Products) and measuring the UV absorption at 595 nm (Cary 600i, Varian).

2.4. Adhesion Characterization. PMaDD-coated membranes were submersed in pH 8 buffer (same buffer composition as used for swelling experiments). The membranes were then ultrasonicated in an ultrasonic bath for 5 min (VWR, model 75D). The samples were removed from the buffer, dried, and then imaged in the SEM described above.

2.5. Functionalization Reaction Conditions. Cysteamine, poly(ethylene glycol), and all solvents were purchased from Sigma Aldrich and used as received. The pol(ethylene glycol) (PEG) had an average molecular weight of 400 g/mol (denoted PEG-400). For cysteamine functionalization, the PMaDD film was reacted in a 0.05 M solution of cysteamine in 2-propanol at 70 °C for 30 min. PMaDD was reacted with PEG-400 in a 10%(v/v) solution of PEG-400 in butyl acetate at 110 °C for 18 h. After the given times, the samples were removed from the reation media and rinsed in clean solvent to remove any unused reactants. The samples were then dried thoroughly in a vacuum oven to remove excess solvent.

To create patterns of PMaDD, TEM grids (G2000HS, SPI Supplies, Inc.) were used as stencil masks. PMaDD films with a thickness of 150 nm were deposited, and the TEM grids were then removed. The PMaDD patterns were functionalized with cysteamine (see above), and commercial CdSe/ZnS core−shell nanoparticles were attached and imaged fluorescently using previously described methods and equipment.[33] The peak emission of the CdSe/ZnS nanoparticles was 610 nm, and the diameter of the CdSe cores was approximately 4.8 nm.

3. Results and Discussion

3.1. Hydrogel Synthesis and Characterization. Poly[maleic anhydride-co-dimethylacrylamide-co-di(ethylene glycol) di(vinyl ether)] (PMaDD) films with average

(30) Tenhaeff, W. E.; Gleason, K. K. *Langmuir* **2007**, *23*, 6624–6630.
(31) McCafferty, E.; Wightman, J. P. *Surf. Interface Anal.* **1998**, *26*, 549–564.
(32) Szczepanski, V.; Vlassiouk, I.; Smirnov, S. *J. Membr. Sci.* **2006**, *281*, 587–591.
(33) Tenhaeff, W. E.; Gleason, K. K. *Thin Solid Films* **2009**, *517*, 3543–3546.

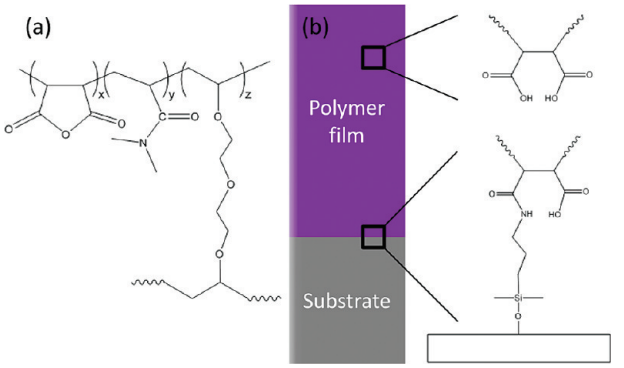

Figure 1. (a) Chemical structure of as-deposited PMaDD network. (b) Illustration of the roles of maleic anhydride at the substrate−film interface and throughout the film bulk.

thicknesses of 150 nm were deposited by iCVD. The copolymer's chemical structure is shown in Figure 1a. The deposition rate measured on silicon was 20 nm/min on average. Prior to deposition, the silicon substrates were functionalized with 3-AMS, yielding primary amine functional groups at the surface. Maleic anhydride groups at the interface between the polymer film and substrate form covalent bonds with the substrate through the reaction between the anhydride and amine functional groups. Without 3-AMS functionalization of the silicon, hydrogel films delaminated from the surface when placed in water. In water, the maleic anhydride throughout the film's bulk hydrolyzed to maleic acid with two ionizable carboxylic acid groups. Figure 1b highlights the role of maleic anhydride at the film−substrate interface and throughout the bulk of the film. Ionization of the maleic anhydride contributed to increasing the swelling of the film because the chemical potential of the ions on the polymer must be equal to the chemical potential of ions in solution. This introduces an ionic term in the Gibbs energy balance for hydrogel equilibrium.[16] The neutral comonomer, *N*,*N*-dimethylacrylamide, was chosen for its ability to absorb large amounts of water; its polymer is considered "super water absorbent."[34] The di(ethylene glycol) di(vinyl ether) (DeDve) component was the cross-linker. The copolymer shown in Figure 1a is a three-dimensional network; di(ethylene glycol) divinyl ether groups of one polymer chain link it to multiple other chains. Through systematic variation of the ratio of monomer and cross-linker flow rates, the cross-linker content in the final copolymer composition was chosen as a compromise between the film's stability in solution and its maximum swelling ratio.

The Fourier transform infrared spectroscopy (FTIR) spectrum of the as-deposited film (Figure 2) provides resolved features of the polymerized Ma and DMAA units. The double carbonyl absorption at 1778 and 1849 cm^{-1} is characteristic of the carbonyl in-phase and out-of-phase stretching of maleic anhydride, while the strong absorption at 1639 cm^{-1} is assigned to the carbonyl stretch of *N*,*N*-dimethylacrylamide.[35] Characteristic peaks of DeDve are obstructed by overlapping absorptions of dimethyl acrylamide and maleic anhydride. The presence of DeDve is verified by the fact that the films did not dissolve in water or tetrahydrofuran, whereas films deposited without DeDve were completely dissolved. Upon placing the films in water, the characteristic FTIR double carbonyl absorption of the anhydride group disappeared. A peak at 1717 cm^{-1}, characteristic of the carbonyl in carboxylic acid groups,[35] and a broad absorption ca. 3500 cm^{-1}, assigned to the O−H stretch, was created (Figure 2a). The possibility of surface reconstruction, which is suggested to occur over a length scale of 1 nm, should not influence the XPS quantification since the XPS sampling depth at 0° is on the order of 10 nm.[36] Moreover, the PMaDD films are cross-linked, which limits independent motion of polymer segments. The high resolution XPS C 1s scans in Figure 2c were used to quantify the composition of the film. The component peak positions were assigned as follows: 289.4 eV to C*(=O)O, 287.7 eV to NC*(=O), 286.1 eV to C*OC and NC*H_3, and 285 eV to CH_x.[37] The composition of the film was quantified by integrating the Gaussion component peaks; the composition was found to be 14% maleic anhydride, 76% *N*,*N*-dimethylacrylamide, and 10% di(ethylene glycol) divinyl ether.

The equilibrium swelling properties of the PMaDD films were characterized as a function of pH using spectroscopic ellipsometry. Prior to measuring the swelling properties, the nongel fraction (uncross-linked polymers) of the film was removed by soaking the samples in 0.1 M NaCl(aq) for 1 h. Dry film thicknesses before and after the soak were measured by ellipsometry. The films lost 40% of their thickness on average; this is the nongel fraction. Only the swelling of the gel portion of the film was measured. The ionic strength of the buffer solution was fixed at 30 mM and buffer strength at 10 mM. The pH dependence of the swelling ratio of PMaDD films is shown in Figure 3a. The degree of swelling (Q) was calculated using $Q = v_{2i}/v_{2s}$, where v_{2i} is the initial volume fraction of polymer (equal to unity for dry, as-deposited films) and v_{2s} is the volume fraction of polymer in the swollen state. The error bars represent the uncertainty in the fit of the ellipsometric model. The swelling ratio clearly increased with pH due to the higher degree of ionization of the hydrogel. The two carboxylic acid groups formed upon hydrolysis of maleic anhydride have unique dissociation constants (pKa1 = 2.8, pKa2 = 6.1),[38] which accounts for the observed swelling response.[16]

A maximum swelling ratio of 11.5 was achieved. Even though it is common for bulk ionic hydrogels to have swelling ratios greater than 100, the swelling ratios are expected to be lower for thin films due to constraints

(34) Künzler, J. F., Hydrogels. In *Encyclopedia of Polymer Science and Technology*; Kroschwitz, J. I., Mark, H. F., Eds.; John Wiley & Sons: Hoboken, NJ, 2003.
(35) Lin-Vien, D.; Colthup, N. B.; Fateley, W. G.; Grasselli, J. G. *The Handbook of Infrared and Raman Characteristic Frequencies of Organic Molecules*; Academic Press: New York, 1991.
(36) Gengenbach, T. R.; Vasic, Z. R.; Chatelier, R. C.; Griesser, H. J. *Plasmas Polym.* **1996**, *1*, 207–228.
(37) Beamson, G.; Briggs, D. *High-Resolution XPS of Organic Polymers The Scientia ESCA300 Database*; John Wiley & Sons: New York, 1992.
(38) Caykara, T. *J. Appl. Polym. Sci.* **2004**, *92*, 763–769.

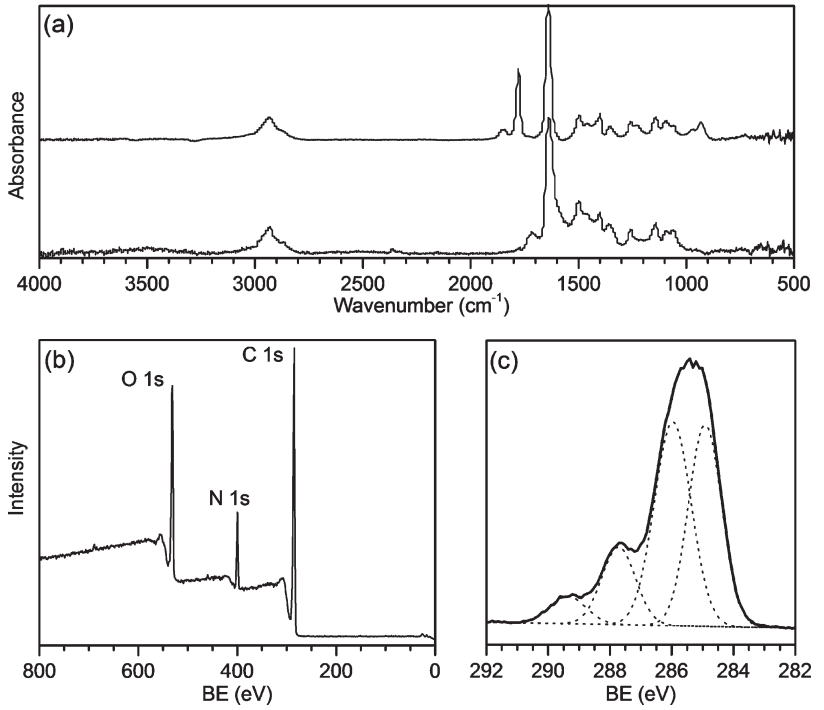

Figure 2. (a) FTIR spectra of as-deposited (top) and hydrolyzed PMaDD (bottom). Note the dramatic difference in intensity of the characteristic peaks of maleic anhydride (at 1778 and 1849 cm^{-1}), while there is little intensity difference in the carbonyl of dimethyacrylamide units (1632 cm^{-1}) (b) XPS survey scans of as-deposited PMaDD and (c) high-resolution spectra of the C 1s region with component peaks fitted to Gaussian distributions for composition quantification.

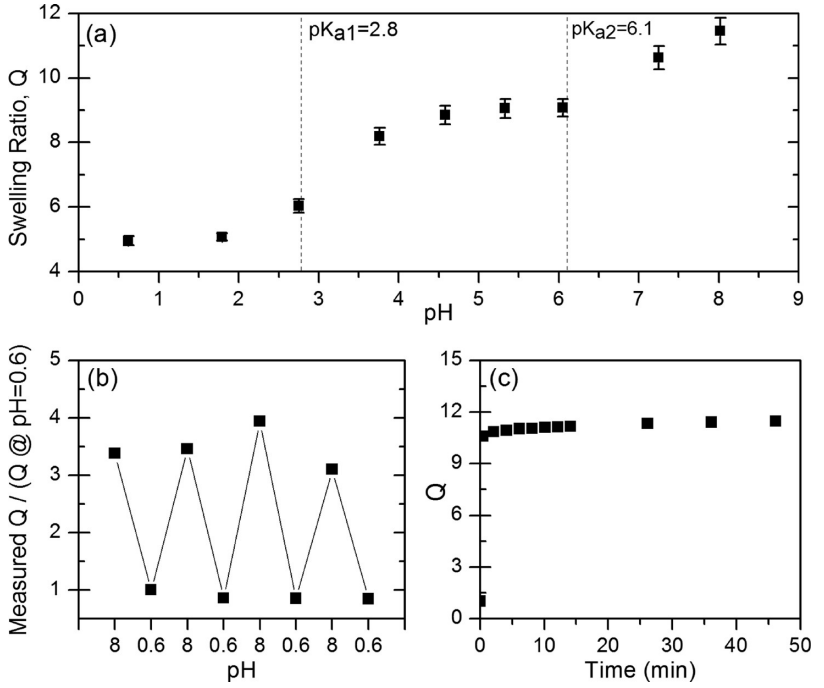

Figure 3. Swelling properties. (a) The pH dependence of swelling of PMaDD films at a fixed ionic strength of 30 mM. Characterization of the (b) reversibility and (c) kinetics of swelling by spectroscopic ellipsometry.

imposed by the solid substrate.[39] These swelling ratios are impressive when compared to previous results for neutral iCVD hydrogel films of poly(2-hydroxyethyl methacrylate), which have swelling ratios <1.5.[40] Hydrogel thin films firmly attached to the substrate that are prepared through other techniques also experience restricted swelling. Four-micrometer-thick films of poly(*N*-isopropyl acrylamide)-based copolymers exhibited swelling ratios of 15,[41] and poly(*N*,*N*-dimethylacrylamide) films had

(39) Toomey, R.; Freidank, D.; Ruhe, J. *Macromolecules* **2004**, *37*, 882–887.
(40) Chan, K.; Gleason, K. K. *Langmuir* **2005**, *21*, 8930–8939.
(41) Harmon, M. E.; Kuckling, D.; Frank, C. W. *Macromolecules* **2003**, *36*, 162–172.

swelling ratios of less than 10.[39] iCVD is a convenient technique to precisely control film thickness, which is important for swelling considerations, because swelling ratios increase with film thickness up to a critical thickness.[41,42] Substrate confinement effects weaken with distance from the surface. Although thickness may affect the swelling, the ionic content of PMaDD, which introduces an ionic term in the Gibbs free energy balance on the hydrogel system, is the primary reason for the high swelling ratios of these films. The high degree of swelling of the PMaDD material is critical for membrane applications. One of the practical limitations of utlrafiltration and nanofiltration membranes is their tendency to foul, in which the pores become blocked. Protein fouling of hydrogel materials generally decreases as water content increases[43] (greater swelling) and their surfaces become more hydrophilic.[44]

The kinetics and reversibility of swelling are also important factors. The reversibility was studied by exposing a film repeatedly to the two pH extremes. The results shown in Figure 3b clearly show the swelling is reversible. Furthermore, the hydrogel swells to 95% of its equilibrium value within 2.5 min (Figure 3c). This indicates the benefit of minimizing film thicknesses. Swelling of hydrogels is a diffusion-limited process (as is diffusion of small molecules through hydrogels); thus, hydrogel nanofilms reach equilibrium swelling on the order of minutes, while bulk gels can take hours.[38]

3.2. Modeling of Permeant Diffusion. The internal pore size is a critical parameter in describing diffusion of solutes through hydrogels. To understand the capability of the PMaDD to serve as a size-selective separation layer, the internal pore structure of the hydrogel and its diffusivity were analyzed. To model the diffusivity of solutes in PMaDD, we propose the Lustig−Peppas model for homogeneous hydrogels, which has been used extensively to model diffusion of drugs and glucose in hydrogels[45−48]

$$\frac{D_g}{D_o} = \left(1 - \frac{r_s}{\xi}\right)\exp\left(-Y\frac{v_{2s}}{1-v_{2s}}\right) \quad (1)$$

where r_s is the hydrodynamic radius of the solute, ξ is the correlation length between cross-links, and v_{2s} is the volume fraction of polymer in the gel. Intuitively, ξ can be described as the mesh size of the hydrogel. Y is a ratio between the volume required for translation movement of the solute to the molar volume of the liquid; setting it to unity is an appropriate approximation.[49] A diffusivity model for solutes in strong polyelectrolytes (also termed heterogeneous hydrogels; see Amsden's review for the distinction between homogeneous and heterogeneous hydrogels[49]) was not used because *N*,*N*-dimethylacrylamide was the primary component in PMaDD. This model (eq 1) shows clearly the ratio of the hydrodynamic radius of the solute to the radius of the internal pores is critical. The mesh size can be calculated using eq 2

$$\xi = v_{2s}^{-1/3} l\sqrt{C_n N} \quad (2)$$

Here l is the length of the C−C bond (0.154 nm), C_n is the characteristic ratio, and N is the number of repeat units between cross-links. N can be calculated using $N = 1/X$, where X is the cross-linking density. The cross-link density can be determined from the XPS analysis above ($X = 0.1$), assuming that the number of physical cross-links (from chain entanglements) is negligible. Because C_n is equal to 8.5 for poly(acrylamide)[50] and 8.4 for poly(methacrylic acid),[51] polymers with repeat units similar to those found in PMaDD, Cn was assumed to be 8.5 for PMaDD. At pH 7 ($v_{2s} = 1/Q = 0.09$), the mesh size of the hydrogel is calculated to be 3.2 nm.

Inserting the calculated pore size and swelling ratio at pH 7 into eq 2, the calculated ratios of diffusion coefficients (D_g/D_0) for glucose ($r_s = 0.36$ nm) and bovine serum albumin ($r_s = 3.6$ nm) are 0.8 and −0.1, respectively. The negative value for the BSA diffusion coefficient is unphysical, implying that the diffusion of BSA is effectively blocked by the hydrogel, which is expected because the hydrodynamic radius of BSA is greater than the hydrogel's mesh size.

3.3. Composite Membrane Characterization. Figure 4 presents an SEM of the commercial alumina membranes before and after being coated with PMaDD via iCVD. It is apparent from Figure 4b that PMaDD formed a blanket layer over the membrane surface. The dry thickness of the hydrogel layer was estimated to be 73 nm from this image and others that were analyzed but not included here. It is difficult to determine from these images the extent of pore fill-in of the PMaDD. The cross-sectional SEM micrographs clearly resolve a smooth overcoat layer and show that the pores remain mostly open. Although it is impossible to rule out some infiltration of the iCVD coating into the pore, the open pores in Figure 4b show that this is not the dominant effect. Previously, the ability of iCVD to bridge openings with limiting pore filling has been deomonstrated.[52] Prevention of significant pore infiltration was achieved by depositing PMaDD under conditions where the P/P_{sat} value of Dmacr was approximately 0.56. P/P_{sat} refers to the partial pressure of the monomer over its saturated partial pressure at the temperature of the

(42) Castellanos, A.; DuPont, S. J.; Heim, A. J.; Matthews, G.; Stroot, P. G.; Moreno, W.; Toomey, R. G. *Langmuir* **2007**, *23*, 6391–6395.
(43) Susanto, H.; Ulbricht, M. *Langmuir* **2007**, *23*, 7818–7830.
(44) Ju, H.; McCloskey, B. D.; Sagle, A. C.; Kusuma, V. A.; Freeman, B. D. *J. Membr. Sci.* **2009**, *330*, 180–188.
(45) Kou, J. H. Transport in Polymer Systems. In *Transport Processes in Pharmaceutical Systems*; Amidon, G. L., Lee, P. I., Topp, E. M., Eds.; Marcel Dekker: New York, 2000.
(46) Lin, C.-C.; Metters, A. T. *Adv. Drug Delivery Rev.* **2006**, *58*, 1379–1408.
(47) Lustig, S. R.; Peppas, N. A. *J. Appl. Polym. Sci.* **1988**, *36*, 735–747.
(48) Podual, K.; Doyle, F. J.; Peppas, N. A. *Polymer* **2000**, *41*, 3975–3983.
(49) Amsden, B. *Macromolecules* **1998**, *31*, 8382–8395.
(50) Bohdanecky, M.; Petrus, V.; Sedlacek, B. *Makromol. Chem., Macromol. Chem. Phys.* **1983**, *184*, 2061–2073.
(51) Ende, M. T. A.; Peppas, N. A. *J. Appl. Polym. Sci.* **1996**, *59*, 673–685.
(52) Baxamusa, S. H.; Im, S. G.; Gleason, K. K. *Phys. Chem. Chem. Phys.* **2009**, *11*, 5227–5240.

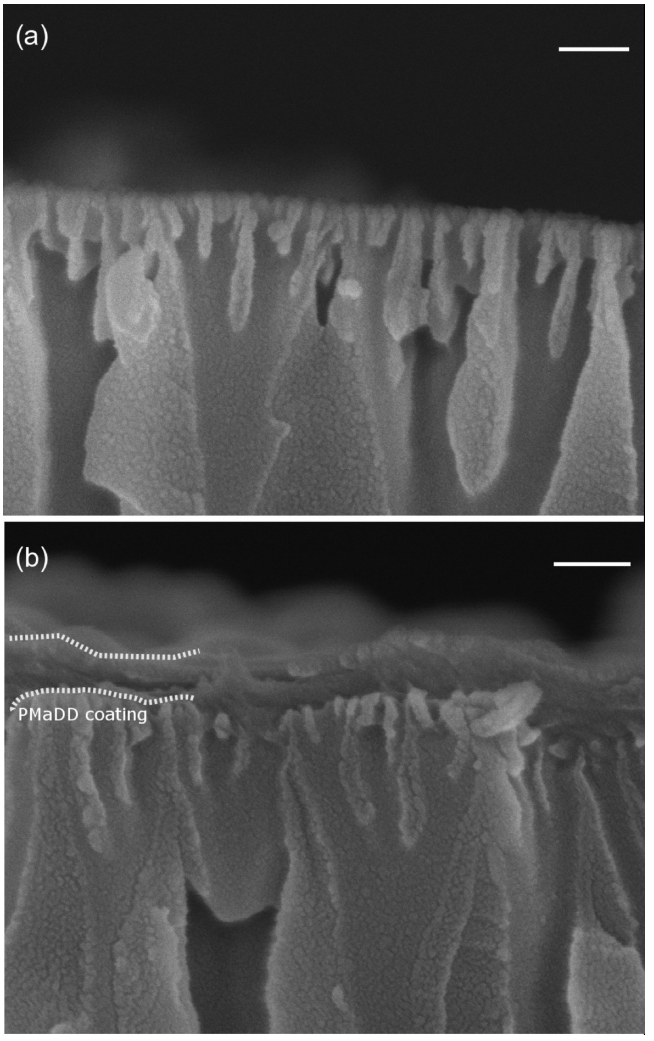

Figure 4. High-resolution SEM images of cross-sections of porous alumina membranes (a) before and (b) after being coated with PMaDD by iCVD. Throughout most of the membrane, the pores are approximately 200 nm in diameter; they reduce to 20 nm at the surface (scale bar = 100 nm). Top down images of the coated membranes are provided in Figure 6a.

substrate during deposition. This partial pressure ratio has been shown to control coating conformality.[53]

Diffusion of glucose and BSA in these composite membranes was measured in a diffusion cell. The kinetics of glucose and BSA diffusion through the alumina membranes with and without the PMaDD layer are presented in Figure 5. Assuming that the volume of the sink is infinite compared to the source, the diffusion kinetics can be modeled using the pseudo steady state approximation in eq 3

$$\ln\left[1-\frac{M_t}{M_1}\right] = \frac{-A\alpha D_i}{lV_1}t \qquad (3)$$

Here M_t is the mass of permeant transferred from source to sink at time t, M_1 is the initial mass of permeant in the source, A is the area available for mass transfer, D_i is the mass transfer coefficient of component i in the composite membrane, l is the thickness of membrane, and V_1 is the

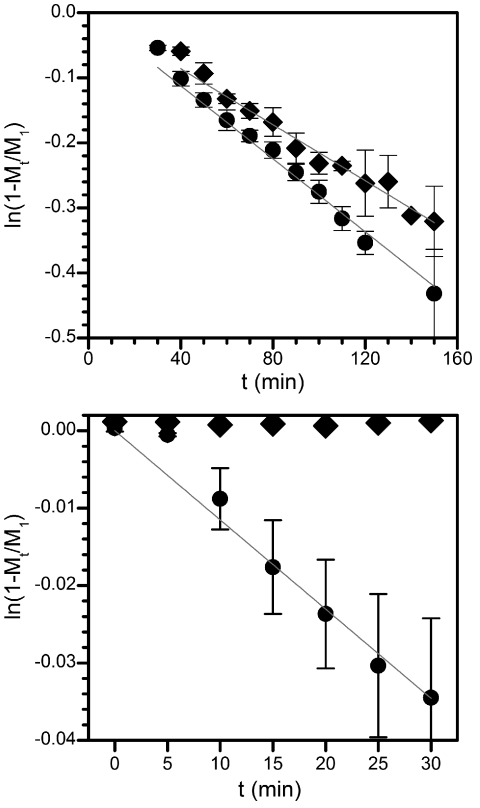

Figure 5. Diffusion kinetics of (a) glucose and (b) BSA through commercially available porous alumina membranes (●) and the same membranes coated with 500 nm PMaDD by iCVD (♦). The pores are 20 nm in diameter at the surface of the alumina membranes.

volume of the source. Clearly, both glucose and BSA diffused through the uncoated porous alumina membranes. Using the slopes of the lines that were linearly regressed to the diffusion data for uncoated membranes in Figure 5, we calculated diffusion constants of 4.3×10^{-7} and 1.8×10^{-7} cm^2 s^{-1} for glucose and BSA, respectively. The disparate time scales for the glucose and BSA diffusion measurements were necessary because of different concentration quantification protocols (see Experimental section for additional details). Figure 5b demonstrates that the PMaDD coating effectively blocks BSA diffusion, as predicted from the models above. There is a slight drop in glucose permeability in the PMaDD-coated membranes (Figure 5a), but the PMaDD clearly blocked the diffusion of BSA. Because the extent of pore infill was unknown, the membrane was not modeled as a laminated structure to determine the diffusion constant of glucose in the PMaDD layer. In future studies of applying iCVD to the synthesis of skin layers, the extent of pore infiltration will be determined and techniques to eliminate it will be developed. A common approach to preventing pore infiltration is prefilling the support layer with polymer or viscous material, such as glycerol, prior to forming the skin layer and then removing the material before using the membrane.[54,55] This

(53) Baxamusa, S. H.; Gleason, K. K. *Chem. Vap. Deposition* **2008**, *14*, 313–318.
(54) Vandezande, P.; Li, X. F.; Gevers, L. E. M.; Vankelecom, I. F. J. *J. Membr. Sci.* **2009**, *330*, 307–318.
(55) Vankelecom, I. F. J.; Moermans, B.; Verschueren, G.; Jacobs, P. A. *J. Membr. Sci.* **1999**, *158*, 289–297.

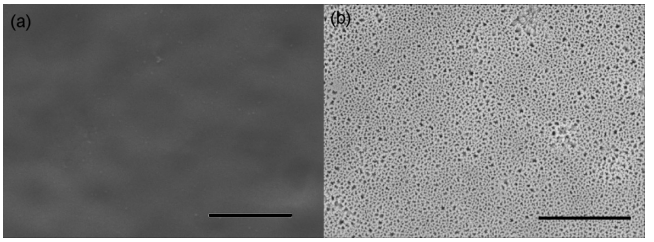

Figure 6. Effect of ultrasonication on PMaDD-coated alumina membranes that (a) were and (b) were not treated with 3-AMS vapors prior to iCVD of PMaDD. The 3-AMS is shown to be critical to PMaDD adhesion (scale bar = 1 μm).

process is compatible with iCVD; it was not performed for this study in order to simplify the fabrication. However, future work will likely employ some variant of this technique, and water permeability of the membranes, which is a critical parameter for practical implementation, will be optimized and reported.

3.4. Stability of Hydrogel Thin Film. The stability of the iCVD coating is also critical. Figure 3a (pH-responsiveness) shows that the polymer is chemically stable in a pH range from less than one to eight. Covalent bonding of PMaDD to the substrate through 3-AMS surface functionalities was required for adhesion stability. 3-AMS was used to covalently bond PMaDD to the alumina membrane. The observation of the successful modulation of the glucose and BSA diffusivities in the PMaDD-coated membranes is strong evidence that PMaDD remained adhered to the alumina.

In commercial or industrial operations, membrane cleaning is an important process. To show that these PMaDD films will be stable to such processes, a vigorous test of adhesion was performed by ultrasonicating the membranes in buffer solution for five minutes. SEM images of ultrasonicated PMaDD-coated membranes with and without 3-AMS exposure before the iCVD step are shown in Figure 6. The PMaDD coating is retained on the membrane that was treated with 3-AMS prior to iCVD, while it delaminated from the untreated membrane to expose the underlying porous surface. The cavitation forces of ultrasonication overcame the physical interaction between the hydrogel and untreated alumina but were not strong enough to break the amide bond created by the reaction of maleic anhydride with the amine of 3-AMS treated alumina.

Furthermore, the coating in Figure 6a, even after ultrasonication, appears to be smooth, showing no trace of the underlying pore structure. Pinholes are not readily apparent, either. By considering this image along with the zero flux of BSA through the PMaDD-coated membranes, it can be concluded that these coatings are free of micrometer-sized pinholes.

3.5. Functionalization of PMaDD. The ability to control the permeability through the mesh properties of the hydrogel has been demonstrated. It is important, as well, to be able to control the interaction of the membrane surface with its environment for fouling considerations. The surface chemistry required to control these interactions will depend on the application, so it is important to

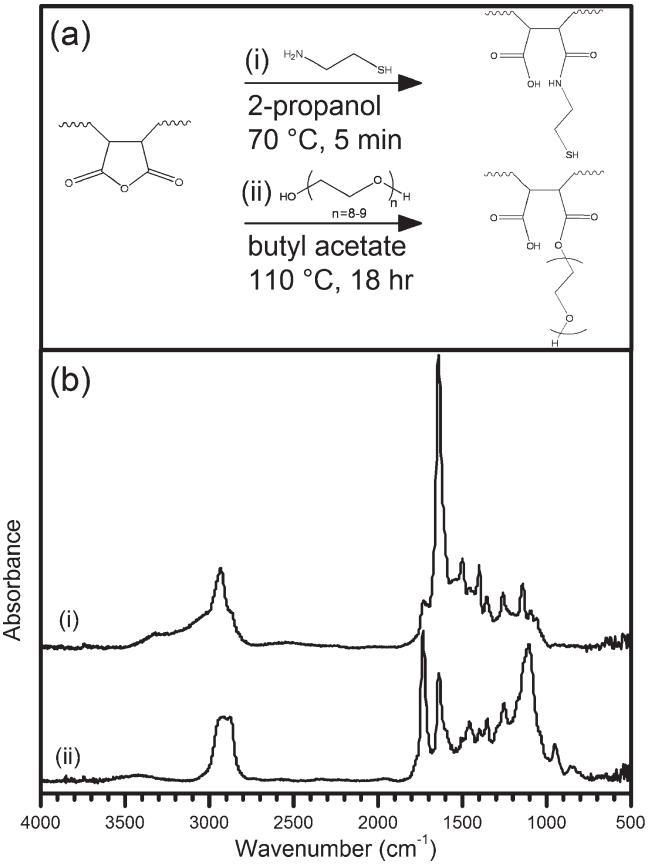

Figure 7. (a) Functionalization of PMaDD with (i) cysteamine and (ii) poly(ethylene glycol) through nucleophilic substitution reactions of the anhydride group. (b) FTIR spectra of the functionalized films reveal the disappearance of the anhydride functionality and confirm the structures of the products shown in (a). Reaction conditions are provided in the Experimental section, and the original spectrum of as-deposited PMaDD is provided in Figure 2a. (The *N*,*N*-dimethylacrylamide and di(ethylene glycol) divinyl ether components in the PMaDD composition are not drawn in (a) because of space constraints.).

have versatile reactive functionality within the membrane. The anhydride in PMaDD is readily functionalized through nucleophilic reactions.[56] The results of functionalizing the anhydride in the PMaDD composition through simple, one-step, uncatalyzed reactions are provided in Figure 7a. The films were functionalized after iCVD but prior to hydrolysis in water. The reactions were chosen to demonstrate the versatility in surface chemistry that can be achieved. Surface thiols have been shown to be protein-adhesive,[57] whereas PEG brushes are widely studied protein-resistant functionalities.[12,17] The PEG molecules had an average molecular weight of 400 g/mol and were denoted PEG-400. PEG functionalization required a longer reaction time and higher temperature because the reaction of hydroxyls with anhydrides is slower than the reaction of amines.[58] Disappearance of the carbonyl absorptions characteristic of anhydride at 1778 and 1852 cm^{-1} indicates that the reaction indeed

(56) Pompe, T.; Zschoche, S.; Herold, N.; Salchert, K.; Gouzy, M. F.; Sperling, C.; Werner, C. *Biomacromolecules* **2003**, *4*, 1072–1079.
(57) Bernkop-Schnurch, A.; Schwarz, V.; Steininger, S. *Pharm. Res.* **1999**, *16*, 876–881.
(58) Trivedi, B. C.; Culbertson, B. M. *Maleic Anhydride*; Plenum Press: New York, 1982.

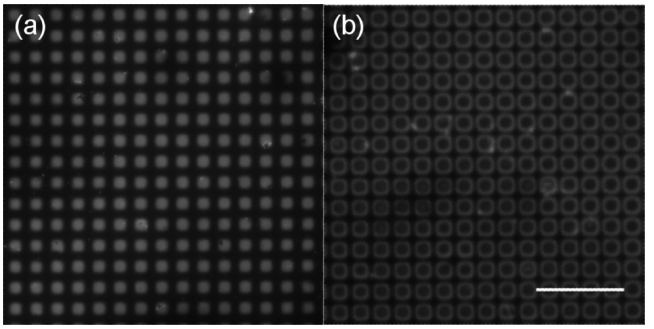

Figure 8. Fluorescent images of PMaDD hydrogel patterns that have been functionalized with cysteamine and linked to CdSe/ZnS nanoparticles. Initially (a) the patterns were dry and then (b) swelled upon immersion in pH 8 buffer (scale bar = 50 μm).

proceeded through a nucleophilic substitution at the anhydride. In the FTIR spectrum of cysteamine functionalized PMaDD, there is a dramatic increase in the absorption at 1638 cm^{-1} and a weak but new absorption ca. 2600 cm^{-1}, which are characteristic of an amide's carbonyl stretch and S−H stretch of thiols, respectively.[35] Although the solvent, 2-propanol, contains a hydroxyl function group that could potentially react to form an ester and contribute features to the FTIR spectrum, it has been shown that the reaction does not occur.[58] The PEG-400 functionalized PMaDD has a new absorption at 1733 cm^{-1} from the carbonyl stretching of the ester that forms upon reaction of hydroxyls with the anhydrides and increased absorptions at 1108 cm^{-1}, characteristic of the C−O—C antisymmetric stretching, and in the hydrocarbon region (2800−3000 cm^{-1}).[35] These spectra are consistent with the product structures drawn in Figure 7a.

In Figure 8a, PMaDD thin films have been patterned using transmission electron microscope (TEM) grids. The TEM grids had 7.5×7.5 μm openings, which were used to define the hydrogel pattern. After the film had been deposited, it was reacted with cysteamine as described in Figure 7a. CdSe/ZnS semiconductor nanoaparticles were readily attached to the thiol groups through a thiol exchange reaction to localize fluorescence to the hydrogel patterns. Because the diameter of the CdSe core (4.8 nm) is larger than the hydrogel mesh size, the CdSe/ZnS remained on the surface and were unable to diffuse into the interior. Fluorescence microscopy was a convenient method to observe hydrogel swelling. Because a carboxylic acid moiety is retained after the functionalization, which increases the swelling due to the ionic term in the Gibbs free energy balance, the hydrogel properties are retained after the functionalization. Visual confirmation of this is provided by the optical micrographs in Figure 8 of dry and swollen hydrogel patterns. The patterns were swollen in the pH 8 buffer described earlier. It is unclear why fluorescence diminishes in the center of the pattern, but it is clear that swelling does occur. It is possible that the CdSe/ZnS nanoparticles adsorbed onto the hydrogels as multilayers, and after swelling, only the nanoparticles attached to the surface remained. Figure 8 confirms that patterning and subsequent surface functionalization of the iCVD ionic hydrogels is possible. These capabilities may find utility in the design of novel membranes, unique surfaces for separation and sensing, or as platforms for cell growth.[59]

4. Conclusion

A highly swellable, pH-responsive ionic hydrogel thin film was synthesized using initiated chemical vapor deposition (iCVD). The capabilities of iCVD in fabricating surface-attached thin ionic hydrogel films have been demonstrated. PMaDD has the highest swelling ratio of any film deposited by iCVD to date; the swelling ratios are more than five times greater than those of other iCVD films. Motivation to use the iCVD synthesis technique has been demonstrated by implementing PMaDD as a size-selective layer on porous anodic alumina substrates to create prototype composite membranes. iCVD enabled the synthesis of defect-free layers with an average thickness of 73 nm on top of porous alumina anisotropic membranes. Little infiltration of the pores by the iCVD film was observed by SEM, but it is likely some does occur. The capability of depositing such thin films with control over conformality should enable the fabrication of many new composite membrane systems. Future work will investigate techniques to optimize membrane permeability and extensively characterize the membrane performance. Moreover, a technique was developed to covalently attach the hydrogel film to the membranes for stability in solution. It is expected that this integration technique is applicable to other membrane materials, such as polyacrylonitrile, cellulose, polysulfone, and polycarbonate, which are commonly employed in ultrafiltration and nanofiltration applications. Reactive functionalities, which are required for the reaction with organosilanes, can be introduced onto the surfaces of polymers through plasma activation.[60] Moreover, iCVD is currently being investigated for the synthesis of high quality films with sub-50 nm thicknesses, which are difficult to achieve by other methods.

Acknowledgment. This material is based upon work supported under a National Science Foundation Graduate Research Fellowship. This research was supported by, or supported in part by, the U.S. Army through the Institute for Soldier Nanotechnologies, under Contract DAAD-19-02-0002 with the U.S. Army Research Office. This work also made use of the MRSEC Shared Facilities supported by NSF Grant DMR-9400334.

(59) Mari-Buye, N.; O'Shaughnessy, S.; Colominas, C.; Semino, C. E.; Gleason, K. K.; Borros, S. *Adv. Funct. Mater.* **2009**, *19*, 1276–1286.
(60) Goddard, J. M.; Hotchkiss, J. H. *Prog. Polym. Sci.* **2007**, *32*, 698–725.